Computers and Structures 89 (2011) 1274–1285

Contents lists available at ScienceDirect

Computers and Structures

journal homepage: www.elsevier.com/locate/compstruc

Nonlinear dynamic structural analysis using dynamic relaxation with zero damping

M. Rezaiee-Pajand *, S.R. Sarafrazi

Department of Civil Engineering, Ferdowsi University of Mashhad, Mashhad, Iran

ARTICLE INFO

Article history:
Received 24 November 2009
Accepted 13 April 2011

Keywords:
Dynamic relaxation
Time-step ratio
Zero damping
Convergence rate
Nonlinear analysis
Dynamic analysis

ABSTRACT

The main idea of the paper is to present a dynamic relaxation algorithm that does not require the damping matrix and velocity terms. The general formulation suggested in this article covers the common DRM as well. In order to verify the ability of the new technique, the obtained static and dynamic solutions are checked with the ones found by the other scheme. When the loads are variable and the behavior of the system is extremely nonlinear, the proposed procedure works efficiently.

© 2011 Elsevier Ltd. All rights reserved.

1. Introduction

The dynamic relaxation method (DRM), as an explicit process, has merit versus the implicit algorithms. The principal virtues are the use of less memory and the elimination of the round-off errors. The DRM converts a static problem to a dynamic one by considering the virtual masses, damping and time steps. If one uses the proper values for the fictitious variables, then the system response will converge to the exact solution. Frankel utilized a finite difference approximation and the linear assumption for the error variation to find the numerical convergence conditions for a system of differential equations [1]. The Frankel method has been applied by other researchers for the solution of elastic problems [2–5]. In addition, there have been many efforts to automatically obtain the DR parameters [6–9]. Recently, investigations on the dynamic relaxation techniques were presented and the merits of this process for solving nonlinear dynamic problems were shown [10–13].

In addition to the fundamental studies, many applications of the DRM have been reported. The researchers, such as Kadkhodayan, Turvey, Salehi and their co-workers, have studied the both geometric nonlinear [14–19] and material nonlinear analyses of the plates [20–22]. Turvey and Salehi have also used the dynamic relaxation process to analyze composite plates [23,24]. Utilizing the adaptive DRM, Oakley et al. considered the analysis of nearly incompressible materials too [25,26]. It should be noted; the dynamic relaxation algorithm searches the stable situation of a structure among the infinitely many unstable cases. It is worth emphasizing, the DR process achieves this target by using a simple algorithm for minimizing the value of the system's total energy. The mentioned property is very useful for analyzing the complicated and very nonlinear problems, such as buckling behavior, and analysis of the tension structures. For example, Ramesh and Krishnamoorthy utilized the DRM to study the post-buckling behavior of truss structures [27,28]. The other researchers performed the buckling analysis of the plates and shells by the DR tactic [29–32].

Another important point is that; the DRM does not require the tangent stiffness matrix. Consequently, it has been used as a simple method for finding the stable state of the cable or tensegrity structures [33–35]. The stable shape of a membrane also can be found using the DR technique [36–41]. It should be added; the real tension structures have many degrees of freedoms. In other words, analyses of these systems require an appreciable time and memory storages. Therefore, the parallel dynamic relaxation algorithms have been also developed [42–44]. Beyond the aforementioned topics, the DR procedure is used for other applications, which require finding the steady state of a system. Among this scatter of subjects, crack propagation [45,46], fluid–structure interaction [47], study granular materials [48] and refinement on the distortion of the membrane elements [49] can be named.

In this paper, a short overview of DR is presented. Afterwards, a general formulation is utilized to evaluate the damping factor via the lowest eigenvalue and the time-step ratio. Consequently, a new method of DR is found by making the critical damping zero. In other words, the parameters of the new algorithm are lumped masses and the time-step ratio. The proposed scheme is an alternative procedure for the common DRM, which uses the critical

* Corresponding author. Tel.: +98 9153130340; fax: +98 5118412912.
E-mail addresses: mrpajand@yahoo.com (M. Rezaiee-Pajand), srsarafrazi@yahoo.com (S.R. Sarafrazi).

0045-7949/$ - see front matter © 2011 Elsevier Ltd. All rights reserved.
doi:10.1016/j.compstruc.2011.04.005

damping and the constant time step. The suggested method can be applied to the dynamic problems. Accordingly, the bases of the dynamic analysis and also some numerical time integration schemes are described. Two strategies of the numerical integration are utilized, which have been recently presented by Bathe [50], and Rezaiee-Pajand and Alamatian [12]. The Wilson-θ [51] and the Newmark-β [52] algorithms are also used. Finally, the capabilities of the new method for analyzing static and dynamic problems are shown using several numerical examples. The responses of the selected integration algorithms are compared with each other. According to the results, using the new formulation will improve the solutions and reduce the total number of the iterations.

2. A short overview of the DRM

A system of linear or nonlinear equations is present whenever a mathematical model is created for a structure. In the stiffness formulation, the displacements **X** are the major unknown variables and the loads **P** are usually known. The stiffness matrix **S** relates these parameters as follows:

$$\mathbf{SX} = \mathbf{P}. \tag{1}$$

In nonlinear systems, the stiffness matrix, and sometimes the forces vector, is related to the displacement vector. There are several iterative techniques used to solve Eq. (1) and one of them is the DRM. This tactic inserts the inertial and damping forces to Eq. (1) to set up the following equation:

$$\mathbf{M}\ddot{\mathbf{X}} + \mathbf{C}\dot{\mathbf{X}} + \mathbf{SX} = \mathbf{P}. \tag{2}$$

In order to solve this equation, two approximations are applied to the DR scheme. The first one approximates the derivatives of the displacements by the central finite difference method. For this purpose, two intervals of the time about t_k should be used. The kth and $(k+1)$th time steps are denoted by τ^k and τ^{k+1}, respectively. Therefore, the velocity $\dot{\mathbf{X}}$ and the acceleration $\ddot{\mathbf{X}}$ are approximated as below:

$$\begin{cases} \dot{\mathbf{X}}^{k+1/2} = \frac{1}{\tau^{k+1}}\left(\mathbf{X}^{k+1} - \mathbf{X}^{k}\right) \\ \dot{\mathbf{X}}^{k} = \frac{1}{2}\left(\dot{\mathbf{X}}^{k-1/2} + \dot{\mathbf{X}}^{k+1/2}\right) \\ \ddot{\mathbf{X}}^{k} = \frac{1}{\tau^{k}}\left(\dot{\mathbf{X}}^{k+1/2} - \dot{\mathbf{X}}^{k-1/2}\right) \end{cases} \tag{3}$$

where, $\dot{\mathbf{X}}^{k\pm1/2}$ is the velocity vector at the middle of the interval time. For simplification, the time step τ^k and the τ^{k+1}/τ^k ratio are shown by h and γ, respectively. By utilizing Eq. (3), Eq. (2) can be expressed in the below non-differential form:

$$\frac{\mathbf{M}}{\gamma h^2}\left[\mathbf{X}^{k+1} - \mathbf{X}^{k} - \gamma\left(\mathbf{X}^{k} - \mathbf{X}^{k-1}\right)\right] + \frac{\mathbf{C}}{2\gamma h}\left[\mathbf{X}^{k+1} - \mathbf{X}^{k} + \gamma\left(\mathbf{X}^{k} - \mathbf{X}^{k-1}\right)\right] + \mathbf{SX}^{k} = \mathbf{P}. \tag{4}$$

One can derive $\mathbf{X}^{k+1}$ from Eq. (4) to obtain the following iterative process:

$$\begin{cases} \mathbf{X}^{k+1} = \mathbf{X}^{k} + \Delta\mathbf{X}^{k+1}, \\ \Delta\mathbf{X}^{k+1} = \gamma\{2h^2[2\mathbf{M} + h\mathbf{C}]\mathbf{R}^{k} + [2\mathbf{M} + h\mathbf{C}]^{-1}[2\mathbf{M} - h\mathbf{C}]\Delta\mathbf{X}^{k}\}, \\ \mathbf{R}^{k} = \mathbf{P} - \mathbf{SX}^{k}. \end{cases} \tag{5}$$

Eq. (5) has convergence ability, if the unknown values of $\mathbf{X}^{0}$, γ, h, **C**, and **M** are properly selected. Mass is a diagonal matrix and has n parameters, where n is the number of degrees of freedom. Researchers determine the mass parameters via some conditions over eigenvalues of $[\mathbf{M}^{-1}\mathbf{S}]$ matrix. They use the Gerschgörin theorem to find the upper bound of the eigenvalues [6,7]. The minimum values of the masses, which guarantee the convergence, are obtained. It should be noted that another scheme is to focus on the viscous dynamic relaxation [53], which eliminates the inertial term from Eq. (2). Other authors focus their efforts towards the selection of the initial displacements [54,55]. It is clear that choosing a good initial displacement vector reduces the total number of the iterations.

The time step and the time-step ratio are other unknowns. It can be shown that the value of the constant time step does not affect the convergence rate. In fact, the constant time step in Eq. (5) makes all the unit of parameter consistence. On the other hand, the damping matrix is usually a factor of the mass matrix in the DRM. The fastest rate of the convergence is obtained when the structure is critically damped. As a result, two unknown variables remain to be defined. They are the critical damping factor and either the optimal time-step ratio or the optimal time step.

Several strategies have been proposed to evaluate the critical damping factor. Most of them use the Rayleigh principle [7,9,56], which can be written in the following form:

$$c_{cr} = 2\sqrt{\frac{\widetilde{\mathbf{X}}^{T}\widetilde{\mathbf{S}}\widetilde{\mathbf{X}}}{\widetilde{\mathbf{X}}^{T}\mathbf{M}\widetilde{\mathbf{X}}}}, \tag{6}$$

where, $\widetilde{\mathbf{X}}$ is a generalized displacement vector. The structure response or difference of displacement between the two sequential steps may be used for $\widetilde{\mathbf{X}}$ [57]. The matrix $\widetilde{\mathbf{S}}$ is usually the stiffness matrix. However, some authors use the diagonal of **S** or the tangential stiffness matrix [8,57]. It should be noted that the Rayleigh quotient usually gives an upper estimation of the critical damping factor [4] and the structure response is over damped. Thus, some researchers tried to estimate a better value for the critical damping factor via the convergence curve [54,58]. These methods have two major difficulties. They require performing several iterations to estimate the critical damping, and the convergence curves do not have simple shapes for the real structures [55].

The optimal time step decreases the total number of iterations. Mathematical relations show that the highest eigenvalue is required to calculate the optimal time step. Therefore, $h = 1$ is usually used. For example, Papadrakakis suggested calculating the optimal time step as follows [6]:

$$h^2_{opt} = \frac{4}{\lambda_1 + \lambda_n}. \tag{7}$$

In this relation, λ_1 and λ_n are the lowest and the highest eigenvalues of $[\mathbf{D}^{-1}\mathbf{S}]$, respectively. It is important to note that the matrix **D** is a diagonal one, and it includes the diagonal terms of the stiffness matrix. In contrast to utilize the highest eigenvalues, Kadkhodayan et al. proposed a process that does not require these values. They used the Rayleigh principle to calculate the damping factor, and also minimized the residual force, as given in the following relation [9]:

$$\mathrm{RFF} = \sum_{i=1}^{ndof}\left(r_i^{k+1}\right)^2 = \sum_{i=1}^{ndof}\left(r_i^{k} - \tau^{k+1}\dot{f}_i^{k+1/2}\right)^2, \tag{8}$$

where, $\dot{f}_i^{k+1/2}$ is the internal force increment at the middle of the time interval for the ith degree-of-freedom and is defined as below:

$$\dot{f}_i^{k+1/2} = \sum_{j=1}^{ndof} s_{ij}\dot{x}_j^{k+1/2}. \tag{9}$$

Moreover, Alamatian suggested minimizing the residual energy in addition to the residual force [59]. This technique is effective using just a few initial iterations. The function of the residual energy is defined by following equation:

$$\Pi_r = \sum_{i=1}^{ndof}\left(\Delta x_i^{k+1} r_i^{k+1}\right)^2 = \left(\tau^{k+1}\right)^2 \sum_{i=1}^{ndof}\left[\dot{x}_i^{k+1/2}\left(r_i^{k} - \tau^{k+1}\dot{f}_i^{k+1/2}\right)\right]^2. \tag{10}$$

It should be mentioned that using the optimal time step leads to a very large or a very small h, after iteration. These values may cause numerical instability. Therefore, experimental limits are required to guarantee process stability. It is worth emphasizing that utilizing the optimal time-step ratio has no such problem. Among the various DR procedures, there is no strategy that eliminates the damping term of Eq. (2). One aim of this effort is to present a DR algorithm that does not require the damping matrix and velocity terms.

3. A general formulation for the DRM

Eq. (2) has several unknown variables and governs a general dynamic system. The finite difference approximation converts Eq. (2) to a simple iterative formula. In general, the iterative scheme requires certain conditions to provide the fastest convergence rate. By transferring from the displacement space to the error space, and assuming linear changes for the errors, Frankel derived the convergence conditions [1]. He defined the error function as $\boldsymbol{\varepsilon}^k = \mathbf{X}^k - \mathbf{X}^*$, where $\mathbf{X}^*$ is the exact solution. Furthermore, a linear relation between two progressive steps was assumed. It is clear that the maximum error value is related to eigenvalues of the coefficients' matrix. If $\boldsymbol{\rho}^k$ denotes the eigenvalues matrix, then the second assumption for the DRM will be derived as below:

$$\boldsymbol{\varepsilon}^{k+1} = \boldsymbol{\rho}^{k+1}\boldsymbol{\varepsilon}^k. \tag{11}$$

In addition, the error ratios of the kth and $(k+1)$th steps are assumed to be equal. Consequently, the third assumption of the dynamic relaxation method is written in the following form:

$$\boldsymbol{\rho}^{k+1} = \boldsymbol{\rho}^k = \boldsymbol{\rho} \;\Rightarrow\; \boldsymbol{\varepsilon}^k = \boldsymbol{\rho}\boldsymbol{\varepsilon}^{k-1}, \quad \boldsymbol{\varepsilon}^{k+1} = \boldsymbol{\rho}\boldsymbol{\varepsilon}^k. \tag{12}$$

One can substitute the error vectors, in place of the displacements, into Eq. (4), and find the following relation:

$$\left\{\frac{\mathbf{M}}{\gamma h^2}\left[\boldsymbol{\rho} - (1+\gamma)\mathbf{I} + \gamma\boldsymbol{\rho}^{-1}\right] + \frac{\mathbf{C}}{2\gamma h}\left[\boldsymbol{\rho} - (1-\gamma)\mathbf{I} - \gamma\boldsymbol{\rho}^{-1}\right] + \mathbf{S}\right\}\boldsymbol{\varepsilon}^k = \mathbf{0}. \tag{13}$$

It should be noted; the mass and damping matrices are related to the stiffness matrix in the DR scheme. Moreover, these matrices must have compatible units. Consequently, the mass and damping matrices are calculated as below:

$$\mathbf{M} = h^2\mathbf{D}, \quad \mathbf{C} = hc\mathbf{D}, \tag{14}$$

where, $\mathbf{D}$ is a diagonal matrix and a function of the stiffness matrix, and c is called the damping factor. It is shown in Appendix A, that the following definition of $\mathbf{D}$ guarantees the convergence of the proposed DR procedure:

$$d_{ii} = \frac{1}{4}\sum_j |S_{ij}|, \tag{15}$$

where, S_{ij} is the general entry of the stiffness matrix $\mathbf{S}$. Eq. (14) show two other assumptions in the DR method, which reduce the large number of unknown variables to $n+2$. Here, n is the number of error ratios related to system's modes. The time-step ratio and the damping factor are two other unknowns. In the sixth assumption of the DRM, the equality $\mathbf{D}^{-1}\mathbf{S}\boldsymbol{\varepsilon}^k = \boldsymbol{\lambda}\boldsymbol{\varepsilon}^k$ is held. The eigenvalues matrix of $[\mathbf{D}^{-1}\,\mathbf{S}]$ is $\boldsymbol{\lambda}$. In other words, $\boldsymbol{\varepsilon}^k$ acts as an eigenvector of $[\mathbf{D}^{-1}\,\mathbf{S}]$ matrix. The last three assumptions for Eq. (13) are used to produce the following equation:

$$\left[\frac{1}{\gamma}\left[\boldsymbol{\rho} - (1+\gamma)\mathbf{I} + \gamma\boldsymbol{\rho}^{-1}\right] + c\frac{1}{2\gamma}\left[\boldsymbol{\rho} - (1-\gamma)\mathbf{I} - \gamma\boldsymbol{\rho}^{-1}\right] + \boldsymbol{\lambda}\right]\boldsymbol{\varepsilon}^k = \mathbf{0}. \tag{16}$$

Moving from the displacement space to the error space converts the DR system into a free oscillation system. It is clear that the non-zero responses for Eq. (16) will be on hand, when the determinant of the coefficients matrices is zero. The result is the below relation:

$$\frac{\rho_i^2 - (1+\gamma)\rho_i + \gamma}{\gamma\rho_i} + c\frac{\rho_i^2 - (1-\gamma)\rho_i - \gamma}{2\gamma\rho_i} = -\lambda_i, \tag{17}$$

where, ρ_i and λ_i are ith diagonal terms of the matrices $\boldsymbol{\rho}$ and $\boldsymbol{\lambda}$, respectively. It should be added that the error ratio is either a complex or a real number. When all ρ_i are complex numbers, the error $\boldsymbol{\varepsilon}$ and the displacement $\mathbf{X}$ are also complex. This means that the response of the structure oscillates, and it is under damped. Conversely, the structure will be over damped if all components of the error ratio are real. Based on this discussion, ρ is written in the following complex form:

$$\rho = \rho_r + id, \;\; \rho_r, d \in R, \quad i = \sqrt{-1}. \tag{18}$$

Substituting the definition (18) into Eq. (17) yields the below relation:

$$\frac{(\rho_r+id)^2 - (1+\gamma)(\rho_r+id) + \gamma}{\gamma(\rho_r+id)} + c\frac{(\rho_r+id)^2 - (1-\gamma)(\rho_r+id) - \gamma}{2\gamma(\rho_r+id)} = -\lambda_i. \tag{19}$$

The separation of the real and the imaginary parts of Eq. (19) gives two relations. In the critical case, and in the over damping one, some or all the error ratios are real numbers. Therefore, to achieve critical damping, one can cancel off the imaginary part of ρ. In other words, d is zero, and the following equations can be obtained:

$$\begin{cases} \rho_i^2(2+c_i) - \rho_i[2\gamma(2-\lambda) + (2+c_i)(1-\gamma)] + \gamma(2-c_i) = 0, \\ \rho_i^2(2+c_i) - \gamma(2-c_i) = 0. \end{cases} \tag{20}$$

However, the maximum value of $||\rho||$ defines the convergence rate. This objective function is added to Eq. (20) to achieve an optimization problem given as below:

$$\begin{cases} \min(\max_i \rho_i^2), \\ \rho_i^2(2+c_i) - \rho_i[2\gamma(2-\lambda) + (2+c_i)(1-\gamma)] + \gamma(2-c_i) = 0, \\ \rho_i^2(2+c_i) - \gamma(2-c_i) = 0, \end{cases} \tag{21}$$

As a result, γ, c_{cr}, ρ_{cr} and the mode number, which defines the maximum value of the error, are the unknown variables. In other words, Eq. (20) shows n damping cases for a specific value of γ. These n points in the $c-\rho$ space are obtained by the following relations:

$$\rho_i = \frac{\alpha_\gamma}{2}(\xi_{\gamma i} \pm \sqrt{\Delta}), \quad \xi_{\gamma i} = 2 - \lambda_{\gamma i}, \quad \Delta = \xi_{\gamma i}^2 - 4\beta_\gamma/\alpha_\gamma^2, \tag{22}$$

$$c_i = \frac{1}{(\gamma+1)^2}\left\{4\gamma\sqrt{\lambda_i[2+\gamma(2-\lambda_i)]} - 2(\gamma-1)(\gamma\lambda_i - \gamma - 1)\right\}. \tag{23}$$

New parameters are defined as below:

$$\alpha_\gamma = \frac{1+\beta_\gamma}{2}, \quad \beta_\gamma = \gamma\beta, \quad \lambda_{\gamma i} = \gamma\frac{\alpha}{\alpha_\gamma}\lambda_i, \quad \alpha = \frac{2}{2+c_i}, \quad \beta = \frac{2-c_i}{2+c_i}. \tag{24}$$

One of the n damping cases causes the highest error value. Comparing the values of $||\rho||$ for the first and the last modes usually give $\max_i \rho_i^2$. In other words, i is usually either 1 or n. If γ changes, the value of $\max_i \rho_i^2$ will change, as well. The optimal time-step ratio will be obtained when $\max_i \rho_i^2$ reduces to a minimum. It can be shown that when γ is less than 1, the maximum value of the error is relevant to λ_1, and $\min\|\rho_n\|$ is less than $\min\|\rho_1\|$. Increasing γ from 1 increases the minimum value of $\|\rho_n\|$, and decreases

$\min \|\rho_1\|$. Consequently, the number of the required iterations decreases until the minimum values of $\|\rho_1\|$ and $\|\rho_n\|$ became the same. After that, λ_n defines the maximum value of the error and the rate of convergence decreases. The value of γ can increase until the maximum value of the error does not become equal or greater than 1. Otherwise, the DR process will diverge. When the damping factors related to λ_1 and λ_n are identical, the error value is reduced to a minimum value. Consequently, using $c|_{\lambda=\lambda_1} = c|_{\lambda=\lambda_n}$ gives the optimal time-step ratio. The result is given by the following equation:

$$\frac{\lambda_1}{\lambda_n}\sqrt{\frac{2(\gamma+1)}{\lambda_1}-\gamma}-\sqrt{\frac{2(\gamma+1)}{\lambda_n}-\gamma}=\frac{1}{2}\left(1-\frac{\lambda_1}{\lambda_n}\right)(1-\gamma). \tag{25}$$

Solving Eq. (25) gives the value of the optimal time-step ratio. One can substitute γ_{opt} and λ_1 into Eq. (23) to obtain c_{cr}. As a result, all of unknown parameters are found. It should be noted that in a few rare cases, the first and the last modes might not be significant and utilizing Eqs. (23) and (25) may reduce the convergence rate.

Finding the optimal time-step ratio requires the highest eigenvalue. Therefore, analysts prefer to use a time-step ratio less than the optimal one. The common choice is the constant time step. When the time-step ratio is 1, Eq. (23) will be converted to the following form:

$$\begin{cases} \max\limits_i \rho_{cri}^2, \\ \rho_{cri}^2(2+c)-2\rho_{cri}(2-\lambda_i)+(2-c_{cri})=0, \\ \rho_{cri}^2(2+c_{cri})-(2-c_{cri})=0. \end{cases} \tag{26}$$

If Eq. (26) are solved simultaneously, the following relations will result:

$$\begin{cases} c_{cr}=\sqrt{\lambda_1(4-\lambda_1)}, \\ \rho_{cr}=\frac{2-c_{cr}}{2-\lambda_1}=\sqrt{\frac{2-c_{cr}}{2+c_{cr}}}. \end{cases} \tag{27}$$

For large structures, λ_1 takes a very small value. Therefore, the value of λ_1^2 compared to $4\lambda_1$ can be ignored and the following approximated relation can be used:

$$c_{cr} \approx 2\sqrt{\lambda_1}. \tag{28}$$

Relation (28) has been utilized by several authors. In fact, the general DR formulation suggested in this investigation covers the common dynamic relaxation method. In the next section, the other special case of Eq. (23) is used. This new procedure does not require damping terms.

4. Proposed method

Finding the optimal time-step ratio from Eq. (25) is too difficult. Utilizing the constant time step is a method to simplify the problem, which is used in the common DRM. The corresponding critical damping for $\gamma = 1$ is presented in Eq. (27). Another approach is to select a damping factor and determine its corresponding time-step ratio. This technique has not been utilized by any researchers so far. A simple value for the critical damping is zero. Therefore, the time-step ratio must be less than one and the maximum error value is related to λ_1. Based on Eq. (23), the critical damping factor is calculated from the following relation:

$$c_{cr}=\frac{1}{(\gamma+1)^2}\left\{4\gamma\sqrt{\lambda_1[2+\gamma(2-\lambda_1)]}-2(\gamma-1)(\gamma\lambda_1-\gamma-1)\right\}. \tag{29}$$

This equation shows that the critical damping is reduced when the value of γ decreases from 1. Therefore, one can find a time-step ratio that corresponds to zero c_{cr}. This value is expressed as below:

$$\gamma=\frac{1}{\left(1+\sqrt{\lambda_1}\right)^2}. \tag{30}$$

Utilizing the last equation along with the zero damping, instead of the critical damping factor, as well as the constant time step, slightly increases the total number of the iterations. The following discussion shows that this increment is negligible for real structures. Numerical experiences show that the number of the iterations is approximately equal to $A/\ln\|\rho\|$. Parameter A is related to the allowable error and initial error in displacement, and can be evaluated from below equation:

$$e^A=\frac{\|\boldsymbol{\varepsilon}^k\|}{\|\boldsymbol{\varepsilon}^0\|}=\sqrt{\frac{(\mathbf{X}^k-\mathbf{X}^*)^T(\mathbf{X}^k-\mathbf{X}^*)}{(\mathbf{X}^0-\mathbf{X}^*)^T(\mathbf{X}^0-\mathbf{X}^*)}}. \tag{31}$$

When the damping factor is zero, the error ratio becomes $\rho = 1/(1+\sqrt{\lambda_1})$. Conversely, the error ratio is given by Eq. (27), when the time step is constant. Fig. 1 shows the differences in the number of the iterations between these two cases for $A = -20$.

As shown in Fig. 1, there is a little difference in the total number of the iterations between the proposed method and the common DR process. In large structures, λ_1 is very small, and increases in the total number of the iterations can be ignored. It should be noted that the zero damping method does not eliminate the requirement for the calculation of the lowest eigenvalue. It is just an alternative scheme for the DRM with a constant time step. The lowest eigenvalue of $\mathbf{G} = [\mathbf{D}^{-1}\,\mathbf{S}]$ is usually calculated using the Rayleigh principle as follows:

$$\lambda_1=\frac{\mathbf{X}^T\mathbf{S}\mathbf{X}}{\mathbf{X}^T\mathbf{M}\mathbf{X}}, \tag{32}$$

The Rayleigh quotient usually gives an upper bound of λ_1. In this case, the first frequency mode is in under the damped condition. Therefore, the response of the structure converges slowly. The simplest scheme for computing a better value of λ_1 is the power iteration technique. The power iteration algorithm can be written as below [60]:

$$\mathbf{u}^1=\{1,1,1,\ldots,1\}^T,$$

$$\begin{cases} \mathbf{v}^k=\mathbf{G}\mathbf{u}^k, \\ \lambda^k=\max(\mathbf{v}^k), \\ \mathbf{u}^{k+1}=\mathbf{v}^k/\lambda^k, \\ k=1,2,3,\ldots \end{cases} \tag{33}$$

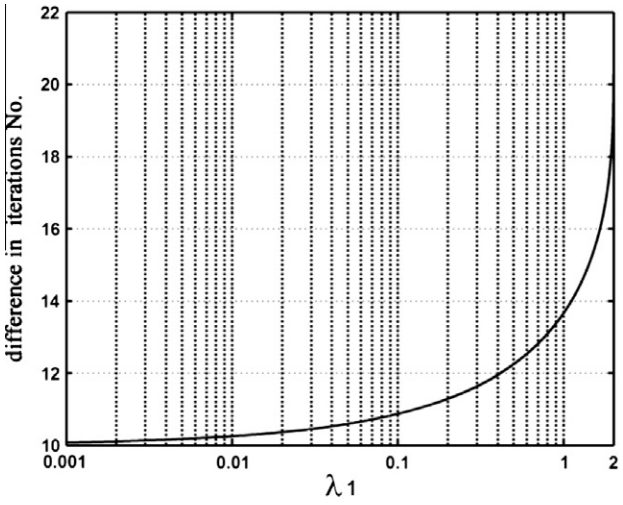

Fig. 1. The effect of the new process on the total number of iterations.

The result converges to the dominant eigenvalue, λ_n. It may also be possible to choose the shift **G**-a**I**, such that $a \geqslant \lambda_n$ [60]. Consequently, the iterative process (33) converges to $\lambda_1 - a$. As it is shown in Appendix A, all eigenvalues of the proposed DR system are less than or equal to four. In other words, it is not necessary to calculate the parameter a, and the value $a = 4$ can be used. The convergence rate of this procedure depends on the λ_2/λ_1 ratio. If the first and the second natural frequencies are close to being equal, the procedures will converge slowly. Nevertheless, from a practical point of view, the power iteration strategy converges faster than the DR technique, and they can be combined together. The proposed scheme uses only one step of the power method in each DR step to update the lowest eigenvalue. It should be noted, utilizing several steps of the power technique in each DR step improves the value of λ_1. However, this process increases the number of computations sharply and decreases the total number of the DR iterations slightly. As a result, the following algorithm is suggested:

(1) $k = 0, \quad a = 4, \quad \mathbf{X}^k = \Delta\mathbf{X}^k = \mathbf{0}, \quad \mathbf{R}^k = \mathbf{P} - \mathbf{S}\mathbf{X}^k, \quad \gamma^k = 1,$
$\mathbf{u}^{k+1} = \{1, 1, 1, \ldots, 1\}^T,$
(2) $\Delta\mathbf{X}^{k+1} = \gamma^k(\mathbf{D}^{-1}\mathbf{R}^k + \Delta\mathbf{X}^k),$
(3) $\mathbf{X}^{k+1} = \mathbf{X}^k + \Delta\mathbf{X}^{k+1}, \quad (\mathbf{R}^{k+1} = \mathbf{P} - \mathbf{S}\mathbf{X}^{k+1} \quad or$
$\mathbf{R}^{k+1} = \mathbf{R}^k - \mathbf{S}\Delta\mathbf{X}^{k+1})$
(4) $if \|\mathbf{R}^{k+1}\| \leqslant \varepsilon_r \quad and \quad \|\Delta\mathbf{X}^{k+1}\| \leqslant \varepsilon_x \quad then \quad STOP,$
(5) $k = k + 1, \quad \mathbf{v}^k = [\mathbf{G} - a\mathbf{I}]\mathbf{u}^k, \quad \lambda^k = \max(\mathbf{v}^k), \quad \mathbf{u}^{k+1} = \mathbf{v}^k/\lambda^k,$
$\lambda_1^k = \lambda^k + a,$
(6) $\gamma^k = \dfrac{1}{(1 + \sqrt{\lambda_1^k})^2},$
(7) GOTO2.

(34)

5. Dynamic analysis

The modal analysis or numerical time integration schemes are common tactics used in the structural dynamic analysis. The modal technique is limited to analyzing linear systems, which include classical damping [61]. On the other hand, numerical integration algorithms are widely applied to both linear and nonlinear analyses. Starting from initial conditions, the unknown variables are calculated step by step in these schemes. Utilizing a proper time step guarantees the stability for finding the true solutions. The dynamic equilibrium equations at time $t_n + \Delta t$ are written below in matrix form:

$$\mathbf{M}\ddot{\mathbf{X}}^{n+1} + \mathbf{C}^{n+1}\dot{\mathbf{X}}^{n+1} + \mathbf{S}^{n+1}\mathbf{X}^{n+1} = \mathbf{P}^{n+1}. \tag{35}$$

The velocities and the accelerations at time t_{n+1} are written in terms of the displacements at this time and the known variables of time t_n. Consequently, an equivalent system of equations is obtained. The unknown variables of this linear or nonlinear system are $\mathbf{X}^{n+1}$. The DR algorithm is appropriate to solve the equivalent system.

Four numerical integration techniques are utilized in this work. These are the second-order method of Bathe [50], the Wilson-θ scheme [51], the 7th-order procedure of Rezaiee-Pajand and Alamatian [12], and the Newmark-β [52] algorithm. The aforementioned methods are denoted by BM2, WTM, IHOA-7, and NLA, respectively. The abilities of these strategies are numerically compared and the merits of the DRM for solving equivalent equations are investigated.

The linear acceleration method of Newmark is a well-known algorithm. The time step should be bounded in this scheme. Wilson applied an additional parameter θ to obtain an unconditional method. It is important to remember that when the value of this parameter is 1, the WTM coincides with the NLA, and the stability of the WTM depends on the time step. However, it is unconditionally stable when the value of θ is greater than 1.37. The optimal value of θ is approximately 1.42. The WTM uses the below relations for the velocities and the accelerations at time $t_n + \theta\Delta t$:

$$\begin{cases} \dot{\mathbf{X}}^{n+\theta} = \frac{3}{\theta\Delta t}(\mathbf{X}^{n+\theta} - \mathbf{X}^n) - 2\dot{\mathbf{X}}^n - 1/2\ddot{\mathbf{X}}^n\theta\Delta t, \\ \ddot{\mathbf{X}}^{n+\theta} = \frac{2}{\theta\Delta t}(\dot{\mathbf{X}}^{n+\theta} - \dot{\mathbf{X}}^n) - \ddot{\mathbf{X}}^n, \end{cases} \tag{36}$$

Recently, Bathe presented a second-order unconditional tactic that has two sub-steps [50]. Using the trapezoidal rule in the first stage, the unknown's variables are evaluated at time $t + \Delta t/2$. Afterwards, the three-point Euler backward scheme is utilized to calculate the nodal variables at time $t + \Delta t$. The BM2 uses the following relations to evaluate the velocities and the accelerations:

$$\begin{aligned} \textit{Stage } 1: & \begin{cases} \dot{\mathbf{X}}^{n+1/2} = \frac{4}{\Delta t}(\mathbf{X}^{n+1/2} - \mathbf{X}^n) - \dot{\mathbf{X}}^n, \\ \ddot{\mathbf{X}}^{n+1/2} = \frac{4}{\Delta t}(\dot{\mathbf{X}}^{n+1/2} - \dot{\mathbf{X}}^n) - \ddot{\mathbf{X}}^n \end{cases} \\ \textit{Stage } 2: & \begin{cases} \dot{\mathbf{X}}^{n+1} = \frac{3}{\Delta t}\mathbf{X}^{n+1} - \frac{4}{\Delta t}\mathbf{X}^{n+1/2} + \frac{1}{\Delta t}\mathbf{X}^n, \\ \ddot{\mathbf{X}}^{n+1} = \frac{3}{\Delta t}\dot{\mathbf{X}}^{n+1} - \frac{4}{\Delta t}\dot{\mathbf{X}}^{n+1/2} + \frac{1}{\Delta t}\dot{\mathbf{X}}^n. \end{cases} \end{aligned} \tag{37}$$

A few higher-order strategies have been presented for numerical integration. Recently, Rezaiee-Pajand and Alamatian suggested a new family, which were related to the formulation previously developed by Zhai [62]. This new family of the algorithms uses the following relation to calculate the increment of acceleration vector [12]:

$$\Delta\ddot{\mathbf{X}}^{n+1} = \eta_0(\ddot{\mathbf{X}}^{n+1} - \ddot{\mathbf{X}}^n) + \sum_{i=1}^{or-1}\eta_i(\ddot{\mathbf{X}}^{n-i} - \ddot{\mathbf{X}}^n), \tag{38}$$

where, or is the order of the proposed integration scheme and η_i are the weighted factors. Eq. (38) is an implicit relation. However, it can be converted to the explicit one by applying $\eta_0 = 0$. The implicit higher-order methods use the below equations for the velocity and the accelerations at time $t_n + \Delta t$:

$$\begin{cases} \dot{\mathbf{X}}^{n+1} = \frac{\eta_0}{\xi_0\Delta t}(\mathbf{X}^{n+1} - \mathbf{X}^n) - \left(1 - \frac{\eta_0}{\xi_0}\right)\dot{\mathbf{X}}^n + \left\{\left(1 - \sum_{i=0}^{or-1}\eta_i\right)\right. \\ \qquad \left. + \frac{\eta_0}{\xi_0}\left(\sum_{i=0}^{or-1}\xi_i - 1/2\right)\right\}\Delta t\ddot{\mathbf{X}}^n + \Delta t\sum_{i=1}^{or-1}(\eta_i - \frac{\eta_0}{\xi_0}\xi_i)\ddot{\mathbf{X}}^{n-i} \\ \ddot{\mathbf{X}}^{n+1} = \frac{1}{\eta_0\Delta t}(\dot{\mathbf{X}}^{n+1} - \dot{\mathbf{X}}^n) - \frac{1}{\eta_0}\left(1 - \sum_{i=0}^{or-1}\eta_i\right)\ddot{\mathbf{X}}^n - \frac{1}{\eta_0}\sum_{i=1}^{or-1}\eta_i\ddot{\mathbf{X}}^{n-i} \end{cases} \tag{39}$$

To find the optimal values of η_i and ξ_i, the accelerations of the previous steps are written in terms of the higher-order derivatives at time t_n. Consequently, the displacements and the velocities at time $t_n + \Delta t$ are obtained in the following form:

$$\begin{cases} \mathbf{X}^{n+1} = \mathbf{X}^n + \Delta t\dot{\mathbf{X}}^n + \sum_{i=0}^{or} a_k\Delta t^{i+2}(\mathbf{X}^{(i+2)})^n \\ \dot{\mathbf{X}}^{n+1} = \dot{\mathbf{X}}^n + \sum_{i=0}^{or} b_k\Delta t^{i+1}(\mathbf{X}^{(i+2)})^n, \end{cases} \tag{40}$$

where, $\mathbf{X}^{(i+2)}$ shows the $(i+2)$th derivatives of the displacement. Furthermore, a_k and b_k are functions of ξ_i and η_i, respectively. Comparing Eq. (40) and the Taylor expansions of the displacement and the velocity, one can find a_k and b_k. The values of ξ_i and η_i are now known. These factors are independent of the system specifications and can be stored in the memory of the computer. For example, for the case of $or = 1$, there are two parameters, $\xi_0 = 1/6$ and $\eta_0 = 1/2$. In this special case, the Rezaiee-Pajand and Alamatian algorithm coincides with NLA. The weighted factors for the accuracy order are reported to be between 1 and 10 [12]. In this work, the seventh-order method from this family is selected for comparison

with the other schemes. This member of the family is not stable for all values of the time steps. A time step of approximately less than $0.25T$ is necessary, where T is the first period of the structure. Eqs. (36), (37), and (39) show the velocity and the acceleration vectors at time $t_n + \Delta t$ in terms of the displacements at that time, and the known variables of the previous steps. The velocity and acceleration vectors can be substituted into dynamic equilibrium Eq. (35) to find $\mathbf{X}^{n+1}$ by solving the following relation:

$$\left[\frac{\xi}{\Delta t^2}\mathbf{M} + \frac{\eta}{\Delta t}\mathbf{C}^{n+1} + \mathbf{S}^{n+1}\right]\mathbf{X}^{n+1} = \mathbf{P}^{n+1} - \mathbf{M}\mathbf{f}_1 - \mathbf{C}\mathbf{f}_2 \sim \mathbf{S}_{eq}\mathbf{X}^{n+1} = \mathbf{P}_{eq}, \quad (41)$$

where, ξ and η are the constant factors and $\mathbf{f}_1$ and $\mathbf{f}_2$ are functions of the displacement, velocity and the acceleration vectors of step n and the previous ones. The values of these parameters depend on the extrapolations' terms of the velocities and the accelerations. In general, Eq. (41) is a nonlinear relation and should be solved using an iterative method. The DRM is a simple and a powerful procedure to solve the linear and nonlinear equations. Because of this merit, the algorithm (34) and the numerical time integration are combined to solve dynamic problems.

Two kinds of the errors may be observed in the dynamic analysis. They are the inaccuracy in the amplitude of the displacements and the period elongation. The values of these errors depend on the time step magnitude, the order of the integration technique, and also the numerical errors that occur when the equivalent equations are solved. It is clear that using the large Δt reduces the number of the integration steps. However, the external forces and earthquake accelerations can change very rapidly with time, and the time step should be chosen small enough to cover the significant points of the force function. In addition, when the time step is large and the structure behavior is nonlinear, solving the equivalent system of the equations causes more numerical errors. The final inaccuracy of the solution is controlled in the DRM. Therefore, when the value of the time step increases, the required number of the iterations also increases. In other words, increasing the value of Δt does not always decrease the overall required calculations.

6. Numerical examples

Five static structures are chosen to verify the proposed algorithm. Specific aspects of the suggested DRM process are studied by solving the first four problems. A large dome truss is then analyzed. According to the prevalent way, the common DRM is compared with the new scheme for all aforementioned structures. It should be noted, the displacements are the major variables in the stiffness method, and the stresses are located in the secondary importance level. Therefore, the displacements' values are considered in these examples. In addition, three other dynamic nonlinear structures will be analyzed after the static problems. The suggested algorithm will be used to analyze the dynamic systems. This study includes all four mentioned numerical time integration strategies. In order to verify the new formulation, the dynamic solutions are checked with the ones obtained by the Rezaiee-Pajand and Alamatian algorithm [11]. This investigation shows the responses errors belong only to the numerical time integration techniques, and the suggested DR procedure has no effect on the solution's accuracy. In other words, utilizing the presented dynamic relaxation tactic with zero damping just affects the total number of the iterations to achieve the nonlinear answers.

6.1. The rod structure

A system having a single degree of freedom is first analyzed. This example consists of a truss shown in Fig. 2. For TR1, the value of AE is 10^7 *lb* and P equals to 1 *lb* [57]. The maximum value of the load factor is 1.5. Furthermore, the geometrical properties of this structure are $H = 1$ and $L_0 \cos\varphi = 100$ *in*. The value of G is 4 for this truss. The minimum eigenvalue and the value of γ are 4 and 1/9, respectively. Consequently, the value of $\|\rho\| is 1/(1+\sqrt{4}) < 1$, and the DR process converges. The number of the iterations shown in Table 1 indicates good results for the rod structure. A comparison of the proposed process and the common DR algorithm in the analysis of the rod structure is also presented in Section 6.5.

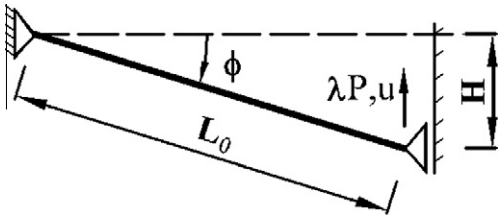

Fig. 2. Truss TR1.

Table 1
The number of iterations for all structures.

Structure	DOFs	Behavior	Methods		
			M1	M2	M3
TR1	1	Linear	12	15	103
		Nonlinear	100	135	750
TR2	42	Linear	736	2057	2103
		Nonlinear	16,576	29,431	30,592
TR3	36	Linear	195	293	285
		Nonlinear	1770	2440	2396
The steel Frame	51	Linear	686	1425	1403
		Nonlinear	5094	10,419	10,303
The dome truss	147	Linear	274	336	314
		Nonlinear	2048	2596	2469

6.2. Truss TR2

Truss TR2 is shown in Fig. 3. This structure is a 28-DOF truss that was solved by Chan and Lau [63,64]. The values of EA, λ and P are 9000, 5 and 1, respectively. The geometric nonlinear analysis of this structure is performed by utilizing the procedure (34). The maximum value of λ is 5 and the incremental load factor is 0.5. As it can be seen in Fig. 4, the load–displacement curve for TR2, which was obtained by Chan and Lau, and the one found by using the new method are equivalent. It is obvious that the proposed algorithm is a very appropriate technique for the nonlinear analysis.

6.3. Truss TR3

In order to study the effects of the time-step ratio on the number of the iterations, a 36-DOF truss is solved. Fig. 5 presents the geometry and loading of TR3. The structural properties are $A = 300$ mm^2, $E = 210{,}000$ N/mm^2, $H = 4$ m and $P = 100$ KN.

TR3 is analyzed for different values of γ. In Fig. 6, the number of the iterations (k) is plotted versus the time-step ratio (γ). The lowest eigenvalue for TR3 is 0.0162. Therefore, Eq. (30) gives 0.787 for γ. According to the Fig. 6, the optimal time-step ratio will be known if Eq. (30) is used. In this formulation, the DR process will diverge, when the value of γ is 1. This is because the damping factor is zero, and the structure will behave as an un-damped free vibration system. In fact, the common DRM with zero damping cannot analyze the structure.

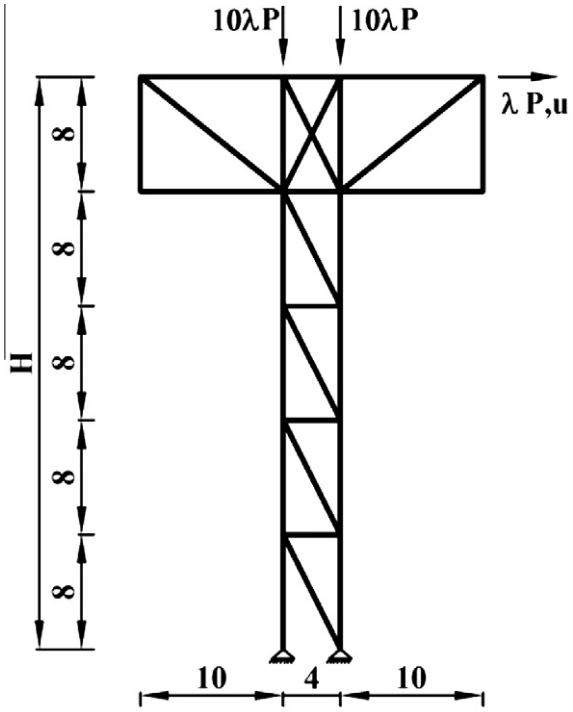

Fig. 3. Truss TR2.

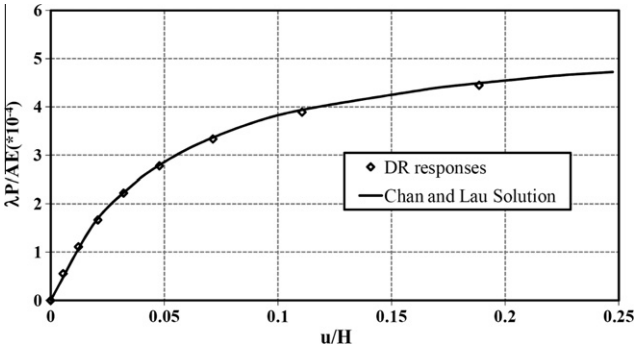

Fig. 4. The load–displacement curve for TR2.

6.4. The steel frame

A steel moment resistant frame is adopted from Barbato's Paper [65] to study the effect of the time-step ratio on the numerical convergence. Fig. 7 shows this structure. Columns and beams are W2150 and W1835, respectively. The modulus of elasticity is 2×10^7 t/m^2.

Three time-step ratios are initially utilized to run the DR process. In the first, γ is calculated based on Eq. (30). It is noted that the lowest eigenvalue for this frame is 0.00185. Consequently, the time-step ratio becomes 0.919. Two other approaches use 0.85 and 0.98 for γ. The norm of the displacement vector **||X||** is plotted versus the iteration number, k, in Fig. 8. It can be seen, when the time-step ratio is less than the optimal case, the structure response will behave as an over damped system. However, values of $\gamma > 0.919$ cause an under damped vibration.

6.5. Comparison study

In this section, some comparisons of the proposed method with the common DR process in solving static problems are presented. For this purpose, all structures that were introduced in the previous sections are analyzed. In addition, the dome truss of Fig. 9 is solved as well. This 3D truss has 147 DOFs [66]. The structural properties are $AE = 10^5$ N and $P = 1000$ N. The maximum value of the load factor for this structure is 1.

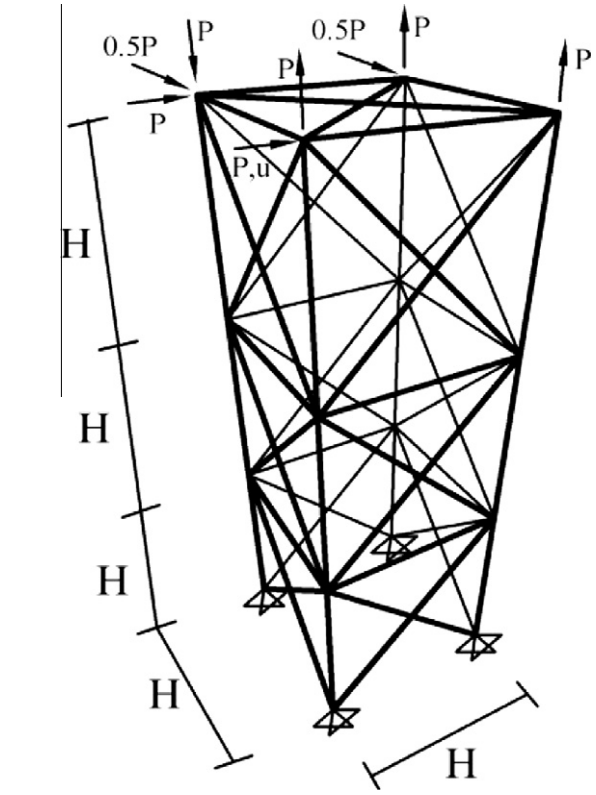

Fig. 5. Truss TR3.

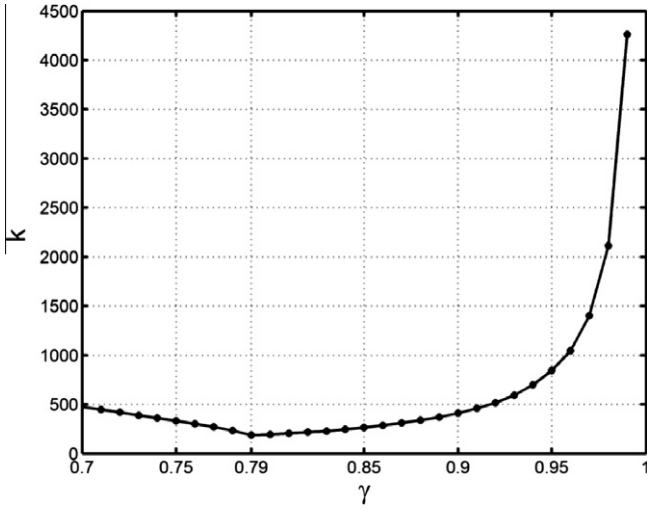

Fig. 6. The curve showing the number of iterations versus γ for TR3.

Both linear and geometric nonlinear analyses are performed for each structure. The incremental load factor for the nonlinear analysis is 0.1 of the final loads. In addition, the allowable error for the residual force is $\varepsilon_r = 10^{-4}$. In other words, the solutions of different strategies for each structure are the same and the total numbers of the required iterations will show the proficiency of the algorithms. The numbers of the iterations to achieve the necessary precision are reported in Table 1. In this Table, M1 and M2 are the DR methods with zero damping. The power iteration scheme is

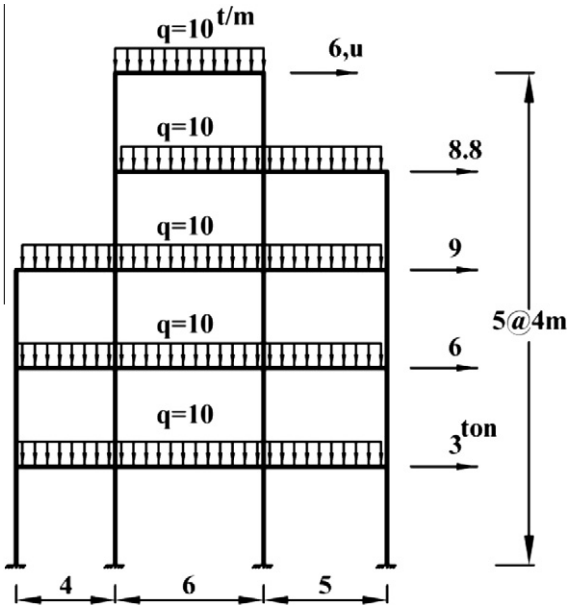

Fig. 7. The steel frame.

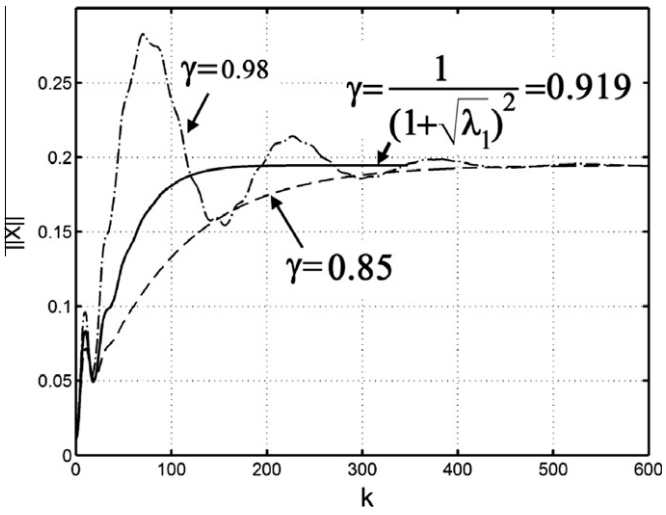

Fig. 8. The convergences curves for the steel frame.

utilized to calculate the lowest eigenvalue in M1. On the other hand, M2 uses the Rayleigh quotient to find λ_1. The common DRM, which was introduced by Underwood [7], is called M3. This tactic assumes $m_{ii} = (1.1/4)\sum_j |s_{ij}|$ and $c = 2\sqrt{\lambda_1} = 2\omega_1$, where ω_1 is the natural frequency of the structure and is evaluated using the Rayleigh principle. In addition, the time-step ratio is 1 for the M3 method. It should be noted, the new schemes presented by the researchers are usually compared with the common DR process.

As it is shown in Table 1, utilizing the same allowable error, the performance of M1 is better than M2 and M2 is almost the same as M3. Therefore, each of the new proposed algorithms has a good ability and can be introduced as an alternative method for the common DRM. According to the results presented in Table 1, the suggested formulation requires a lesser number of the iteration. By paying just a little cost and using the power iteration procedure to calculate λ_1 causes an appreciable improvement in the convergence rate. It is important to note that too many iterations in the analysis of the TR2 roots on the vicious nonlinear behavior of the structure. In fact, more than 50% of the iterations belong to the last three load increments. In addition, there is a significant difference between the iteration number of M3 and other procedures for the SDOF truss. This is because the value of the mass in the Underwood method is far from exact. The proper mass of SDOF system is $2S/4$ in the common DRM. However, Underwood assumed $m = 1.1S/4$.

6.6. The geodesy dome

TR5 is a 3D truss that has 156 elements and 111 DOFs. This structure is shown in Fig. 10. The sections' areas of all members are 2 in^2 (1290.32 mm^2). The modulus of elasticity and density are 3×10^4 Ksi (2.068×10^5 MPa) and 7.77×10^{-4} lb/in^3 (8303 Kg/m^3), respectively. The weights of the elements are ignored and a concentrated load is applied on the top of the dome for 0.5 s. All base joints of the dome are fixed. A nonlinear dynamic analysis of this structure is performed by the suggested technique.

Four numerical integration strategies are applied to analyze TR5. They are: BM2, WTM with $\theta = 1.42$, NLA and IHOA-7. The nonlinear analyses are done for the three time steps 0.01, 0.001 and 0.0001 s. The vertical displacement of the top truss joint is plotted versus the time in Figs. 11 and 12.

As shown in Fig. 11, the behavior of the IHOA-7 and the NLA techniques are the same in this example. They are unstable for $\Delta t = 0.001$s, and the time-displacement curves for these schemes coincide at $\Delta t = 0.0001$ s. In other words, the higher-order terms in the IHOA-7 algorithm had no more effect on the analysis of TR5, since the required time step is too small. The first period of

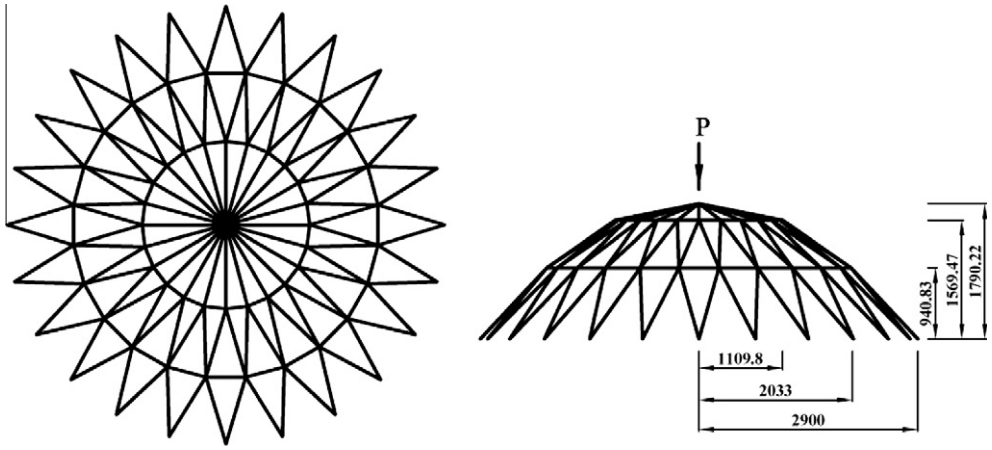

Fig. 9. The dome truss.

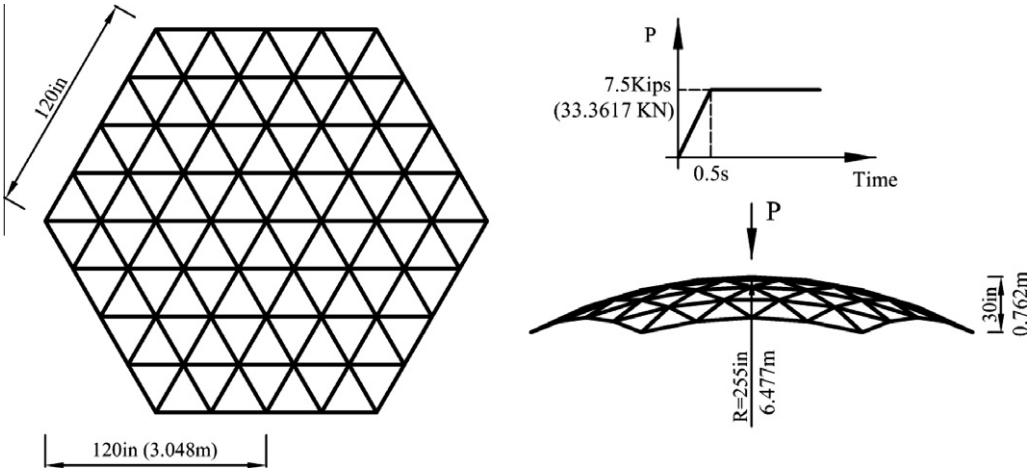

Fig. 10. The TR5 truss.

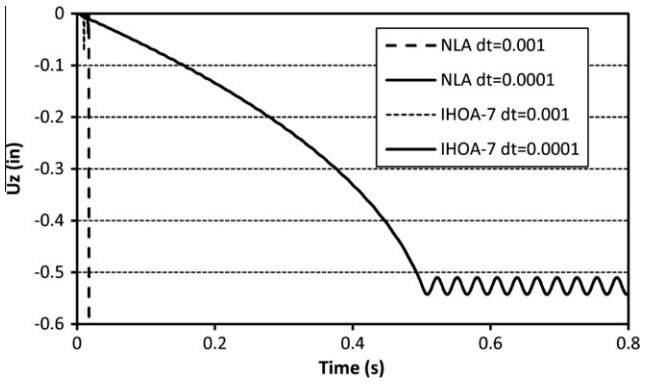

Fig. 11. Time–displacement curve for TR5.

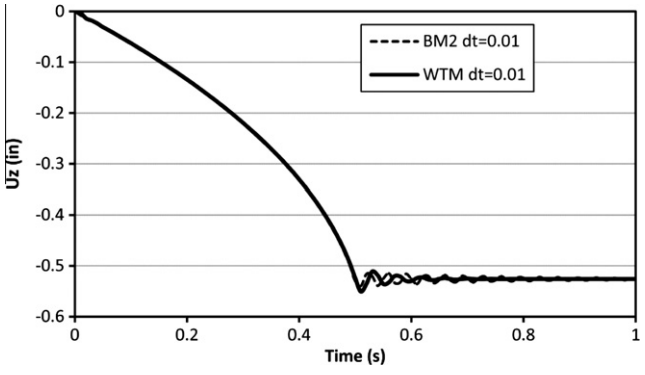

Fig. 12. Time–displacement curve for TR5.

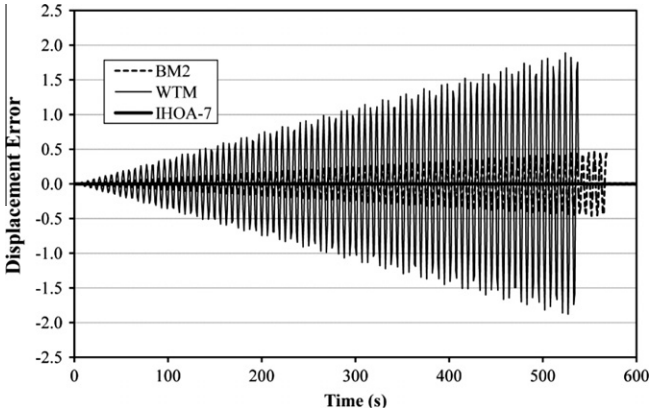

Fig. 13. The error magnitude of *x*.

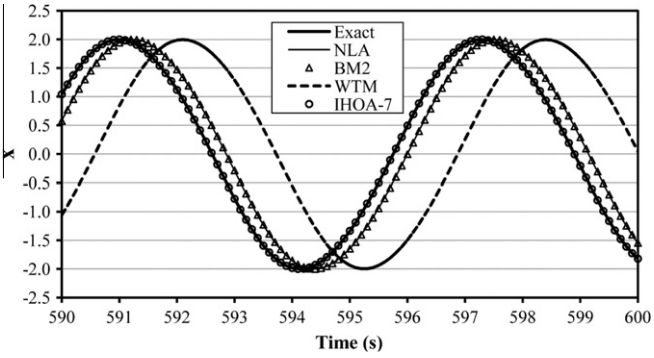

Fig. 14. The curves of *x*.

this structure is $T = 0.016$ s. Therefore, the NLA and the IHOA-7 are unstable even for $\Delta t = .06255T$.

Fig. 12 shows that the BM2 and the WTM methods give approximately identical results. Furthermore, they are stable even for $\Delta t = .6255T$. This example also shows the merit of the proposed DR algorithm, when the loads are variable and the behavior of the system is extremely nonlinear.

6.7. Van-Der-Pol equation

Numerical time integration causes two kinds of errors. One is the error in the displacement magnitude. If the value of the error increases too much, the response of a structure will be unstable. Incorrect estimation of the structural period is the other error. This causes a difference in phase amplitude between the numerical and the exact solutions of the system. In this example, the phase difference error is studied by solving the Van-Der-Pol equation. The differential equation of this problem and its approximate analytical solution are written below:

$$\ddot{x} - \mu(1 - x^2)\dot{x} + x = 0, \quad x^0 = 2, \quad \dot{x}^0 = 0, \quad \mu = 0.1,$$

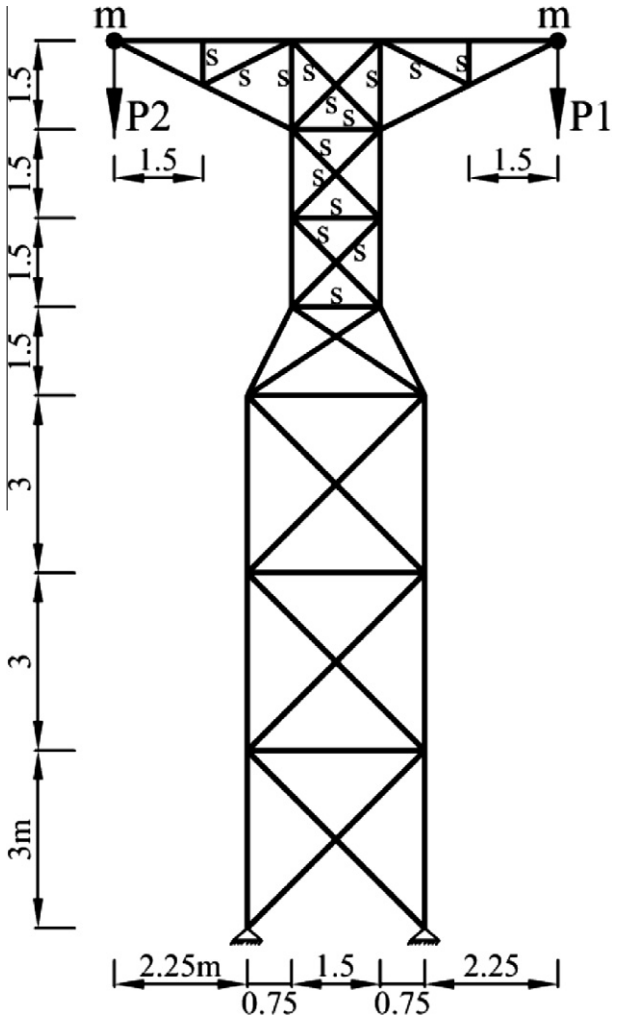

Fig. 15. The pylon structure (TR6).

$$x = (x^0 - \frac{\mu^2}{8})\cos(\omega t) + \frac{3}{4}\mu\sin(\omega t) + \frac{3}{16}\mu^2\cos(3\omega t) - \frac{1}{4}\mu\sin(3\omega t) - \frac{1}{16}\mu^2\cos(5\omega t),$$

$$\omega = 1 - \frac{\mu^2}{16}.$$

Using $\Delta t = 0.1$ s, the Van-Der-Pol equation is solved by all mentioned methods, which were utilized in solving the geodesy dome. The difference between the near exact solution and the numerical integration schemes' versus the time is plotted in Fig. 13.

Fig. 13 shows that the maximum values of the error belong to the WTM. The NLA and the BM2 cause similar errors. Therefore, the curve of NLA is not plotted. However, the error of the higher-order scheme is insignificant. The errors in this example arise from phase differences. To show this type of the error, the time–displacement curves from 590 to 600 s are plotted in Fig. 14. This figure indicates that all tactics give good results for the displacement magnitude. However, the numerical schemes estimate the period of the system with some errors. Among all the time integration techniques tested, the higher-order terms of the integration reduce this type of the error.

6.8. The pylon structure

TR6 is a 2D model of an electricity pylon and has 40 DOFs. The material properties of this structure are: $\rho = 7850\ \mathrm{Kg/m^3}$ and $E = 2 \times 10^5$ MPa. The truss members are constructed from two kinds of the sections. As shown in Fig. 15, the section areas, which are denoted by s, are 600 $\mathrm{mm^2}$, and the rest is equal to 3000 $\mathrm{mm^2}$. Two lumped masses, $m = 150$ Kg, and two concentrated forces are applied at the top-left and the top-right joints of the structure. The concentrated loads change with time according to the below equations:

$$P1 = 120\sin(\pi t/2) \quad KN,$$

$$P2 = 120\cos(\pi t/2) \quad KN.$$

It should be noted that the weights of the members are ignored. Moreover, the consistent mass matrix for each member is utilized to assemble the structural mass matrix.

Linear dynamic analyses are performed for the pylon structure by using the BM2, WTM, NLA and the IHOA-7 methods. The main period of this truss is 0.145 s. However, the external forces cause much more rapid oscillation. There is not an exact solution available for this problem. Therefore, the solutions are compared with the answers of the BM2, when a fine time step, such as $\Delta t = 0.0001$ s, is utilized. As shown in Figs. 16 and 17, the BM2 and the WTM give good results even for the time step of 0.01 s. However, the NLA and IHOA-7 are unstable even for $\Delta t = 0.001$ s.

The analysis of this structure shows that the stability of the numerical time integration method is more important than the order of the integration algorithm. However, analyzing TR6 with the

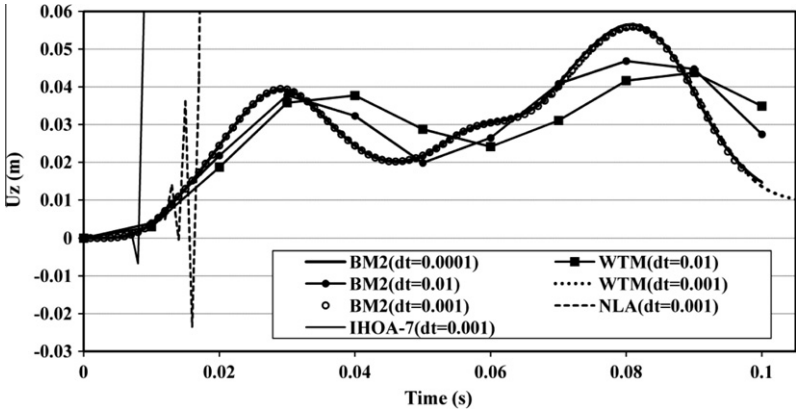

Fig. 16. The vertical displacement of the truss top-right joint.

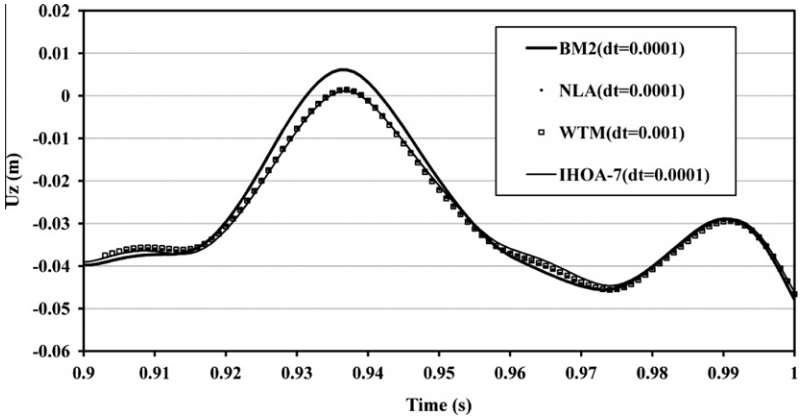

Fig. 17. The vertical displacement of the truss top-right joint between times 0.9 and 1 s.

BM2 and the WTM requires a fine time step, like $\Delta t = 0.007T$.On the other hand, the IHOA-7 needs a smaller Δt. Previous results from the geodesy dome showed that the IHOA-7 was stable with $\Delta t = 0.006, T$.

7. Conclusions

A new DR method is presented that has no damping terms. This study shows that the proper time-step ratio guarantees the convergence of the proposed formulation. Furthermore, utilizing the time-step ratio in the analysis means that a very small time step is no longer necessary. The suggested algorithm is an alternative process for the common dynamic relaxation tactic, which uses critical damping, and a constant time step. Using one step of the power iterative strategy to update the value of the lowest eigenvalue will improve the new process and reduce the total number of the iterations. Furthermore, the suggested approach is shown to be applicable to nonlinear dynamic problems. Besides the study on the ability of the DRM, the merits of two new numerical time integration schemes, and two other older ones, are compared. The results show that the stability of the time integration technique in the proposed nonlinear structural analysis algorithm is more important than its order.

Appendix A. The proof of the stability for the proposed method

The upper bound of the highest eigenvalue of $\mathbf{G} = [\mathbf{D}^{-1}\,\mathbf{S}]$ matrix can be calculated by Gerschgörin theorem, as follows:

$$|\lambda_i - g_{ii}| \leqslant \sum_{j\neq i} |g_{ij}| \quad \Rightarrow \quad 0 < \lambda_i \leqslant \sum_j |g_{ij}| = \frac{1}{d_{ii}} \sum_j |s_{ij}|. \tag{42}$$

Substituting Eq. (15) into Eq. (42), leads to $0 < \lambda_i \leqslant 4$. On the other hand, the error ratio of the suggested process is obtained by using Eqs. (22) and (30) and zero damping factor

$$\rho = 1/\left(1 + \sqrt{\lambda_1}\right). \tag{43}$$

Consequently, when the eigenvalues are bounded between zero and four, the relation $1/3 \leqslant \rho < 1$ is satisfied. In other words, the value of the error ratio is less than one. As a result, the proposed algorithm always converges.

References

[1] Frankel SP. Convergence rates of iterative treatments of partial differential equations. Math Tables Aids Comput 1950;4:65–75.
[2] Brew JS, Brotton M. Non-linear structural analysis by dynamic relaxation. Int J Numer Methods Eng 1971;3:463–83.
[3] Wood WL. Note on dynamic relaxation. Int J Numer Methods Eng 1971;3:145–7.
[4] Bunce JW. A note on estimation of critical damping in dynamic relaxation. Int J Numer Methods Eng 1972;4:301–4.
[5] Cassell AC, Hobbs RE. Numerical stability of dynamic relaxation analysis of non-linear structures. Int J Numer Methods Eng 1976;10:1407–10.
[6] Papadrakakis M. A method for automatic evaluation of the dynamic relaxation parameters. Comput Methods Appl Mech Eng 1981;25:35–48.
[7] Underwood P. Dynamic relaxation. In: Belytschko T, Hughes TJR. (editors), In computational method for transient analysis. Amsterdam: Elsevier; 1983. pp. 245–65.
[8] Qiang S. An adaptive dynamic relaxation method for nonlinear problems. Comput Struct 1988;30:855–9.
[9] Kadkhodayan M, Alamatian J, Turvey GJ. A new fictitious time for the dynamic relaxation (DXDR) method. Int J Numer Methods Eng 2008;74:996–1018.
[10] Rezaiee-Pajand M, Taghavian-Hakkak M. Nonlinear analysis of truss structures using dynamic relaxation. Int J Eng 2006;19:11–22.
[11] Rezaiee-Pajand M, Alamatian J. Nonlinear dynamic analysis by dynamic relaxation method. Struct Eng Mech 2008;28:549–70.
[12] Rezaiee-Pajand M, Alamatian J. Implicit higher-order accuracy method for numerical integration in dynamic analysis. J Struct Eng ASCE 2008;134: 973–85.
[13] Rezaiee-Pajand M, Alamatian J. Numerical time integration for dynamic analysis using a new higher order predictor–corrector method. Eng Comp 2008;25:541–68.
[14] Turvey GJ, Salehi M. DR large deflection analysis of sector plates. Comput Struct 1990;34:101–12.
[15] Salehi M, Shahidi A. Large deflection analysis of elastic sector Mindlin plates. Comput Struct 1994;52:987–98.
[16] Turvey GJ, Salehi M. Large deflection analysis of eccentrically stiffened sector plates. Comput Struct 1998;68:191–205.
[17] Salehi M, Aghaei H. Dynamic relaxation large deflection analysis of non-axisymmetric circular viscoelastic plates. Comput Struct 2005;83:1878–90.
[18] Ramesh G, Krishnamoorthy CS. Geometrically non-linear analysis of plates and shallow shells by dynamic relaxation. Comput Methods Appl Mech Eng 1995;123:15–32.
[19] Kobayashi H, Turvey GJ. On the application of a limiting process to the dynamic relaxation analysis of circular membranes, circular plates and spherical shells. Comput Struct 1993;48:1107–16.
[20] Frieze PA, Hobbs RE, Dowling PJ. Application of dynamic relaxation to the large deflection elasto-plastic analysis of plates. Comput Struct 1978;8:301–10.
[21] Turvey GJ, Salehi M. Elasto-plastic response of uniformly loaded sector plates: full-section yield model predictions and spread of plasticity. Comput Struct 2001;79:2335–48.
[22] Kadkhodayan M, Zhang LC. A consistent DXDR method for elastic–plastic problems. Int J Numer Methods Eng 1995;38:2413–31.
[23] Turvey GJ, Salehi M. Annular sector plates: comparison of full-section and layer yield predictions. Comput Struct 2003;83:2431–41.
[24] Salehi M, Sobhani AR. Elastic linear and non-linear analysis of fiber-reinforced symmetrically laminated sector Mindlin plate. Comput Struct 2004;65:65–79.
[25] Oakley DR, Knight NF. Adaptive dynamic relaxation algorithm for non-linear hyperelastic structures Part I. Formulation. Comput Methods Appl Mech Eng 1995;126:67–89.
[26] Oakley DR, Knight NF. Adaptive dynamic relaxation algorithm for non-linear hyperelastic structures Part II. Single-processor implementation. Comput Methods Appl Mech Eng 1995;126:91–109.
[27] Ramesh G, Krishnamoorthy CS. Post-buckling analysis of structures by dynamic relaxation. Int J Numer Methods Eng 1993;36:1339–64.
[28] Ramesh G, Krishnamoorthy CS. Inelastic post-buckling analysis of truss structures by dynamic relaxation method. Int J Numer Methods Eng 1994;37:3633–57.
[29] Frieze PA, Dowling PJ. Interactive buckling analysis of box sections using dynamic relaxation. Comput Struct 1978;9:431–9.

[30] Kadkhodayan M, Zhang LC, Sowerby R. Analyses of wrinkling and buckling of elastic plates by DXDR method. Comput Struct 1997;65:561–74.
[31] Pasqualino IP, Estefen SF. A nonlinear analysis of the buckle propagation problem in deepwater pipelines. Int J Solids Struct 2001;38:8481–502.
[32] Toulios M, Caridis PA. The effect of aspect ratio on the elastoplastic response of stiffened plates loaded in uniaxial edge compression. Comput Struct 2002;80:1317–28.
[33] Shea K, Fest E, Smith FC. Developing intelligent tensegrity structures with stochastic search. Adv Eng Inf 2002;16:21–40.
[34] Han S, Lee K. A study of the stabilizing process of unstable structures by dynamic relaxation method. Comput Struct 2003;81:1677–88.
[35] Domer B, Fest E, Lalit V, Smith FC. Combining dynamic relaxation method with artificial neural networks to enhance simulation of tensegrity structures. J Struct Eng ASCE 2003;129:672–81.
[36] Wakefield DS. Engineering analysis of tension structures: theory and practice. Eng Struct 1999;21:680–90.
[37] Tang G, Ma B, Chu W. Dynamic renormalization-group approach to growing surfaces with point-defects. Physica A 2000;282:355–61.
[38] Adriaenssens SML, Barnes MR. Tensegrity spline beam and grid shell structures. Eng Struct 2001;23:29–36.
[39] Hegyi D, Sajtos I, Geiszter G, Hincz K. Eight-node quadrilateral double-curved surface element for membrane analysis. Comput Struct 2006;84:2151–8.
[40] Topping BHV, Ivanyi P. Computer aided design of cable-membrane structures. Saxe-Coburg Publications; 2007.
[41] Ong CF, Wakefeld DS, Barnj MR. Interactive graphic cad for tension structures. Comput Struct 1991;41:1305–12.
[42] Oakley DR, Knight NF, Warner DD. Adaptive dynamic relaxation algorithm for non-linear hyperelastic structures Part III. Parallel implementation. Comput Methods Appl Mech Eng 1995;126:111–29.
[43] Topping BHV, Khan AI. Parallel schemes for dynamic relaxation. Eng Comp 1994;11:513–48.
[44] Ivanyi P, Topping BHV. Parallel dynamic relaxation form-finding. In Innovative computational methods for structural mechanics. Stirlingshire, UK: Saxe-Coburg Publications; 1999. pp. 127–47.
[45] Gerstle WH, Xie M. FEM modeling of fictitious crack propagation in concrete. J Eng Mech ASCE 1992;118:416–34.
[46] Yang HY, Wang ML, Chen XM. Structural finite-element analysis with new interface model. J Eng Mech ASCE 1997;123:276–85.
[47] Küttler U, Wall WA. Fixed-point fluid–structure interaction solvers with dynamic relaxation. Comput Mech 2008;43:61–72.
[48] Bardet JP, Proubet J. Adaptive dynamic relaxation for statics of granular materials. Comput Struct 1991;39:221–9.
[49] Wood RD. A simple technique for controlling element distortion in dynamic relaxation form-finding of tension membranes. Comput Struct 2002;80:2115–20.
[50] Bathe KJ. Conserving energy and momentum in nonlinear dynamics: a simple implicit time integration scheme. Comput Struct 2007;85:437–45.
[51] Wilson EL, Farhoomand I, Bathe KJ. Nonlinear dynamic analysis of complex structures. Earthquake Eng Struct Dyn 1973;1:241–52.
[52] Newmark NM. A method of computation for structural dynamics. J Eng Mech Div ASCE 1959;85:67–94.
[53] Zienkiewicz OC, Lohner R. Accelerated 'relaxation' or direct solution? Future prospects for FEM. Int J Numer Methods Eng 1985;21:1–11.
[54] Alwar RS, Ramachandra Rao N, Subba Pao M. An alternative procedure in dynamic relaxation. Comput Struct 1975;5:271–4.
[55] Zhang LC, Kadkhodayan M, Mai YW. Development of the maDR method. Comput Struct 1994;52:1–8.
[56] Zhang LC, Yu TX. Modified adaptive dynamic relaxation method and its application to elastic–plastic bending and wrinkling of circular plates. Comput Struct 1989;34:609–14.
[57] Crisfield M. Non-linear finite element analysis of solids and structures, Advanced topics, vol. 2, John Wiley & Sons Ltd.; 1997.
[58] AL-Shawi FAN, Mardirosian AH. An improved dynamic relaxation method for the analysis of plate bending problems. Comput Struct 1987;27:237–40.
[59] Alamatian J. Numerical integration for structural analysis. Department of Civil Engineering, Ferdowsi University, Mashhad, Iran, 2007 (in Persian).
[60] Krishnamoorthy EV, Sen SK. Numerical algorithms-computations in science and engineering. New Delhi: Affiliated East-West Press; 1991.
[61] Chopra Anil K. Dynamics of structures: theory and applications to earthquake engineering. second ed. New Jersey, USA: Prentice-Hall; 2006.
[62] Zhai WM. Two simple fast integration methods for large-scale dynamic problems in engineering. Int J Numer Methods Eng 1996;39:4199–214.
[63] Chan ASL, Lau TB. Further development of the reduced basis method for geometric nonlinear analysis. Comput Methods Appl Mech Eng 1987;62:127–44.
[64] Tatar M. Nonlinear structural analysis based on static path. Department of Civil Engineering, Ferdowsi University, Mashhad, Iran; 2002 (in Persian).
[65] Barbato M, Conte JP. Finite element response sensitivity analysis: a comparison between force-based and displacement-based frame element models. Comput Methods Appl Mech Eng 2005;194:1479–512.
[66] Papadrakakis M, Pantazopoulos G. A survey of quasi-Newton with reduced storage. Int J Numer Methods Eng 1993;36:1573–96.